Cell Reports
Medicine

Report

Cross-Sectional Evaluation of Humoral Responses against SARS-CoV-2 Spike

Graphical Abstract

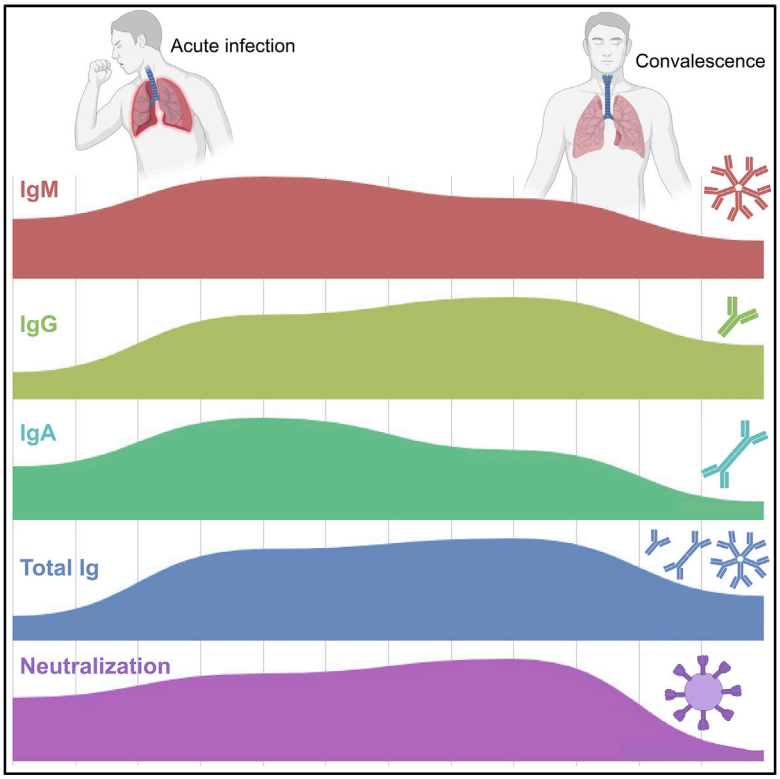

Highlights

- Antibodies against SARS-CoV-2 Spike correlate with COVID-19 severity
- RBD-specific IgM and IgA decline more rapidly than IgG
- SARS-CoV-2 neutralizing antibodies are elicited within 2 weeks of infection
- Neutralizing antibodies decline significantly after resolution of the infection

Authors

Jérémie Prévost, Romain Gasser, Guillaume Beaudoin-Bussières, ..., Renée Bazin, Michel Roger, Andrés Finzi

Correspondence

andres.finzi@umontreal.ca

In Brief

Prévost et al. report a cross-sectional study on a cohort of 106 COVID-19 patients and show that most infected individuals are able to elicit a sustained antibody response over time. However, plasma neutralizing capacity wanes after infection resolution, but its implication on protection from re-infection remains unknown.

Prévost et al., 2020, Cell Reports Medicine *1*, 100126
October 20, 2020
https://doi.org/10.1016/j.xcrm.2020.100126

CellPress

Cell Reports Medicine

CellPress
OPEN ACCESS

Report

Cross-Sectional Evaluation of Humoral Responses against SARS-CoV-2 Spike

Jérémie Prévost,[1,2,20] Romain Gasser,[1,2,20] Guillaume Beaudoin-Bussières,[1,2,20] Jonathan Richard,[1,2,20] Ralf Duerr,[3,20] Annemarie Laumaea,[1,2,20] Sai Priya Anand,[1,4] Guillaume Goyette,[1] Mehdi Benlarbi,[1] Shilei Ding,[1] Halima Medjahed,[1] Antoine Lewin,[5] Josée Perreault,[5] Tony Tremblay,[5] Gabrielle Gendron-Lepage,[1] Nicolas Gauthier,[6] Marc Carrier,[7] Diane Marcoux,[8] Alain Piché,[9] Myriam Lavoie,[10] Alexandre Benoit,[11] Vilayvong Loungnarath,[12] Gino Brochu,[13] Elie Haddad,[2,15,18] Hannah D. Stacey,[19] Matthew S. Miller,[19] Marc Desforges,[14,15] Pierre J. Talbot,[14] Graham T. Gould Maule,[16] Marceline Côté,[16] Christian Therrien,[17] Bouchra Serhir,[17] Renée Bazin,[5] Michel Roger,[1,2,17] and Andrés Finzi[1,2,4,21,*]

[1]Centre de Recherche du CHUM, Montreal, QC H2X 0A9, Canada
[2]Département de Microbiologie, Infectiologie et Immunologie, Université de Montréal, Montreal, QC H2X 0A9, Canada
[3]Department of Pathology, New York University School of Medicine, New York, NY 10016, USA
[4]Department of Microbiology and Immunology, McGill University, Montreal, QC H3A 2B4, Canada
[5]Héma-Québec, Affaires Médicales et Innovation, Québec, QC G1V 5C3, Canada
[6]Hôpital Sacré-Cœur de Montréal, Montreal, QC H4J 1C5, Canada
[7]Hôpital Cité-de-la-Santé, Laval, QC H7M 3L9, Canada
[8]Hôtel-Dieu de Lévis, Lévis, QC G6V 3Z1, Canada
[9]Centre Hospitalier Universitaire de Sherbrooke, Sherbrooke, QC J1H 5H4, Canada
[10]CIUSSS du Saguenay-Lac-Saint-Jean, Hôpital de Chicoutimi, Chicoutimi, QC G7H 5H6, Canada
[11]Hôpital de Verdun, Montreal, QC H4G 2A3, Canada
[12]CHU de Québec, Hôpital Enfant-Jésus, Quebec, QC G1J 1Z4, Canada
[13]CIUSSS de la Mauricie-et-du-Centre-du-Québec, Trois-Rivières, QC G9A 5C5, Canada
[14]INRS-Institut Armand Frappier, Laval, QC H7V 1B7, Canada
[15]CHU Ste-Justine, Montreal, QC H3T 1C5, Canada
[16]Department of Biochemistry, Microbiology and Immunology, and Center for Infection, Immunity, and Inflammation, University of Ottawa, Ottawa, ON K1H 8M5, Canada
[17]Laboratoire de Santé Publique du Québec, Institut national de santé publique du Québec, Sainte-Anne-de-Bellevue, QC H9X 3R5, Canada
[18]Département de Pédiatrie, Université de Montréal, Montreal, QC H3T 1C5, Canada
[19]Micheal G. DeGroote Institute for Infectious Disease Research, Master Immunology Research Centre, Department of Biochemistry and Biomedical Sciences, McMaster University, Hamilton, ON L8N 3Z5, Canada
[20]These authors contributed equally
[21]Lead Contact
*Correspondence: andres.finzi@umontreal.ca
https://doi.org/10.1016/j.xcrm.2020.100126

SUMMARY

SARS-CoV-2 is responsible for the coronavirus disease 2019 (COVID-19) pandemic, infecting millions of people and causing hundreds of thousands of deaths. The Spike glycoproteins of SARS-CoV-2 mediate viral entry and are the main targets for neutralizing antibodies. Understanding the antibody response directed against SARS-CoV-2 is crucial for the development of vaccine, therapeutic, and public health interventions. Here, we perform a cross-sectional study on 106 SARS-CoV-2-infected individuals to evaluate humoral responses against SARS-CoV-2 Spike. Most infected individuals elicit anti-Spike antibodies within 2 weeks of the onset of symptoms. The levels of receptor binding domain (RBD)-specific immunoglobulin G (IgG) persist over time, and the levels of anti-RBD IgM decrease after symptom resolution. Although most individuals develop neutralizing antibodies within 2 weeks of infection, the level of neutralizing activity is significantly decreased over time. Our results highlight the importance of studying the persistence of neutralizing activity upon natural SARS-CoV-2 infection.

INTRODUCTION

The first step in the replication cycle of coronaviruses is viral entry. This process is mediated by their trimeric Spike (S) glycoproteins. Similar to that of SARS-CoV, the S glycoprotein of SARS-CoV-2 interacts with angiotensin-converting enzyme 2 (ACE2) as its host receptor.[1–3] During entry, the S binds the host cell through interaction between its receptor binding domain (RBD) and ACE2 and is cleaved by cell surface proteases or endosomal cathepsins,[1,4,5] triggering irreversible conformational changes in

Table 1. Cross-Sectional SARS-CoV-2 Cohort Clinical Characteristics

Group	n	Days after Onset of Symptoms (median; day range)	Age (median; age range)	Sex	
				Male (n)	Female (n)
T1	24	3 (2–7)	50 (31–94)	11	13
T2	20	11 (8–14)	64 (34–90)	9	11
T3	26	22 (16–30)	40 (20–93)	10	16
T4	9	36 (31–43)	39 (24–87)	3	6
Convalescent	27	41 (23–52)	37 (19–69)	20	7

the S protein and enabling membrane fusion and viral entry.[6,7] The SARS-CoV-2 S is very immunogenic, with RBD representing the main target for neutralizing antibodies (Abs).[8–11] Humoral responses are important for preventing and controlling viral infections.[12,13] However, little is known about the chronology and durability of the human Ab response against SARS-CoV-2.

RESULTS

Here, we analyzed serological samples from 106 SARS-CoV-2-infected individuals at different times post-symptom onset and 10 uninfected individuals for their reactivity to SARS-CoV-2 S glycoprotein and cross-reactivity with other human CoVs (HCoVs), as well as virus neutralization. Samples were collected from COVID-19-positive individuals starting on March 2020 or healthy individuals before the COVID-19 outbreak (COVID-19 negative). Cross-sectional serum samples (from different patients at different time points) (n = 79) were collected at the hospital from individuals presenting typical clinical symptoms of acute SARS-CoV-2 infection (Table 1). All patients were positive for SARS-CoV-2 by RT-PCR on nasopharyngeal specimens. The average age of the infected patients was 55 years old, and samples were from 33 males and 46 females. Samples were classified into 4 time points after symptom onset: 24 (11 males, 13 females) were obtained at 2–7 days (T1; median = 3 days), 20 (9 males, 11 females) between 8–14 days (T2; median = 11 days), 26 (10 males, 16 females) between 16–30 days (T3; median = 22 days), and 9 (3 males, 6 females) between 31–43 days (T4; median = 36 days). Additionally, samples were obtained from 27 convalescent donors (20 males, 7 females; median = 41 days) who were diagnosed with or tested positive for COVID-19 and had a complete resolution of symptoms for at least 14 days. These donors reported symptoms of a different intensity (from mild/moderate to severe), although none of them were hospitalized for COVID-19.

We first evaluated the presence of RBD-specific immunoglobulin G (IgG) and IgM Abs by ELISA.[14,15] The level of RBD-specific IgM peaked at T2 and was followed by a stepwise decrease over time (T3, T4, and convalescent) (Figure 1). Three-fourths of the patients had detectable anti-RBD IgM 2 weeks after the onset of symptoms. Similarly, 85% of patients in T2 developed anti-RBD IgG, reaching 100% in convalescent patients. In contrast to IgM, the levels of RBD-specific IgG peaked at T3 and remained relatively stable after complete resolution of symptoms (convalescent patients).

We next used flow cytometry to examine the ability of sera to recognize the full-length SARS-CoV-2 S expressed at the cell surface. Briefly, 293T cells expressing SARS-CoV-2 S glycoproteins were stained with samples, followed by incubation with secondary Abs recognizing all Ab isotypes (including IgG, IgM, and IgA). As presented in Figure 2, 54.2% of the sera from T1 already contained SARS-CoV-2 full S-reactive Abs. Interestingly, most patients from T2, T3, T4, and convalescent groups were found to be seropositive, which is in agreement with results of a previous report.[16] The higher seropositivity detected by flow cytometry is most likely due to the detection of Abs with multiple specificity and of different isotypes simultaneously. Ab levels targeting the SARS-CoV-2 S significantly increased from T1 to T2/T3 and remained relatively stable thereafter. As expected, the levels of Abs recognizing the full S correlated with the presence of both RBD-specific IgG and IgM (Figure S1). We also evaluated potential cross-reactivity against the closely related SARS-CoV S. None of the COVID-19-negative samples recognized the SARS-CoV S. Although the reactivity of COVID-19-positive samples to SARS-CoV S was lower than that for SARS-CoV-2 S, it followed a similar progression and significantly correlated with their reactivity to SARS-CoV-2 full S or RBD protein (Figures 2 and S1). This result indicates that SARS-CoV-2-elicited Abs cross-react with human *Sarbecovirus*. This finding was also observed with another *Betacoronavirus* (OC43) but not with *Alphacoronavirus* (NL63, 229E) S glycoproteins, suggesting a genus-restrictive cross-reactivity (Figures 2C and S1). Notably, anti-OC43 RBD Abs did not fluctuate upon SARS-CoV-2 infection (Figure S2). Therefore, this differential cross-reactivity could be explained by the high degree of conservation in the S protein fusion machinery, particularly in the S2 subunit among *Betacoronavirus* members.[17–19]

We next measured the capacity of patient samples to neutralize pseudoparticles bearing SARS-CoV-2 S, SARS-CoV S, or vesicular stomatitis virus G (VSV-G) glycoproteins using 293T cells stably expressing ACE2 as target cells (Figures 3 and S3). Neutralizing activity, as measured by the neutralization half-maximum inhibitory dilution (ID_{50}) or the neutralization 80% inhibitory dilution (ID_{80}), was detected in most patients within 2 weeks after the onset of symptoms (T2, T3, T4, and convalescent patients) (Figure 3). SARS-CoV-2 neutralization was specific because no neutralization was observed against pseudoparticles expressing VSV-G. The capacity to neutralize SARS-CoV-2 S-pseudotyped particles significantly correlated with the presence of RBD-specific IgG/IgM and anti-S Abs (Figure S4). Although the percentage of patients eliciting neutralizing Abs against SARS-CoV-2 S remained relatively stable 2 weeks after disease symptom onset (T2, T3, T4, and convalescent patients), neutralizing Ab titers significantly decreased after 1 month of infection (T4) or after the complete resolution of symptoms, as observed in the convalescent patients (Figures 3G and 3H). Similarly to RBD-specific IgM, levels of RBD-specific IgA were also found to peak at T2 and decrease over time (Figure S4B). However, RBD-specific IgM levels displayed a stronger correlation with neutralization activity than that of RBD-specific IgG and

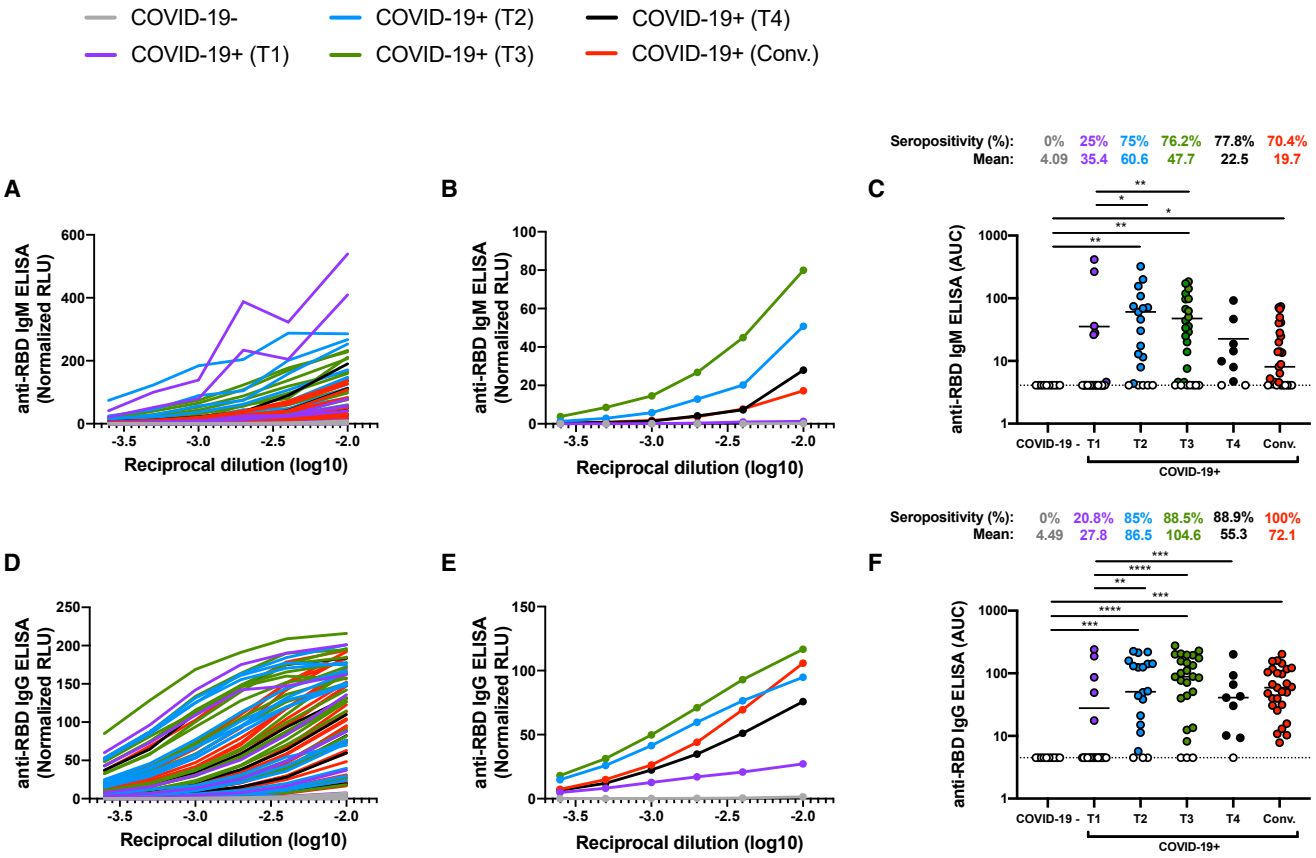

Figure 1. Detection of SARS-CoV-2 RBD-Specific IgM and IgG over Time

Indirect ELISA was performed using recombinant SARS-CoV-2 RBD and incubated with samples from 10 COVID-19-negative or 106 COVID-19-positive patients at different times after symptoms onset (T1, T2, T3, T4, and convalescent). Anti-RBD binding was detected using anti-IgM-HRP (A–C) or anti-IgG-HRP (D–F). Relative light units (RLUs) obtained with BSA (negative control) were subtracted and further normalized to the signal obtained with the anti-RBD CR3022 mAb present in each plate. Data in graphs (A) and (D) represent RLUs performed in quadruplicate. Curves depicted in (B) and (E) represent the mean RLUs detected with all samples from the same group. Undetectable measures are represented as white symbols, and limits of detection are plotted. (C, F) Areas under the curve (AUCs) were calculated based on RLU datasets shown in (A) and (D) using GraphPad Prism software. Statistical significance was tested using Kruskal-Wallis tests with a Dunn's post-test (*$p < 0.05$; **$p < 0.01$; ***$p < 0.001$; ****$p < 0.0001$).

IgA, suggesting a more prominent role for IgM, but the decrease in IgA could also contribute to the loss of neutralization activity, as recently suggested.[20] Cross-reactive neutralizing Abs against SARS-CoV S protein (Figure 2B) were also detected in some SARS-CoV-2-infected individuals, but with significantly lower potency, and they waned over time. We note that around 40% of convalescent patients did not exhibit any neutralizing activity. This finding suggests that the production of neutralizing Abs is not a prerequisite for the resolution of the infection and that other arms of the immune system could be sufficient to control the infection in an important proportion of the population.

To determine whether underlying correlation patterns among Ab responses detected in SARS-CoV-2-infected individuals were associated with demographic and clinical parameters, we performed a comprehensive correlation analysis, focusing on data from the acute stages of SARS-CoV-2 infection (T1, T2, T3, and T4) (Figures 4 and S5). Donors from these groups were matched for age, sex, and disease severity (Figure S5). The statistical analysis revealed a prominent cluster of positive correlations between SARS-CoV-2, SARS-CoV, and OC43 S Ab binding, SARS-CoV-2 neutralization, and days post-symptom onset (Figure S6). The cluster became evident in a linear correlation analysis involving all study parameters (Figure S6A). Of interest, clinical parameters formed another cluster of positive correlations between respiratory symptoms, hospitalization, oxygen supplementation, and intensive care unit (ICU) admission (Figure S6A). The presence of respiratory symptoms and hospitalization also correlated with age of the infected patients. We also used chord diagrams to study the network of immunological and clinical correlation pairs longitudinally (from T1 to T4); these diagrams consisted of linear correlation analysis summarized in a circular plot, with chords indicating correlations between the 2 connected parameters: red color indicates positive correlation, blue color inverse correlation, and chord width corresponds to significance (the broader, the more significant). We observed an increased diversification of associations between the parameters (Figures 4B–4E), Associations

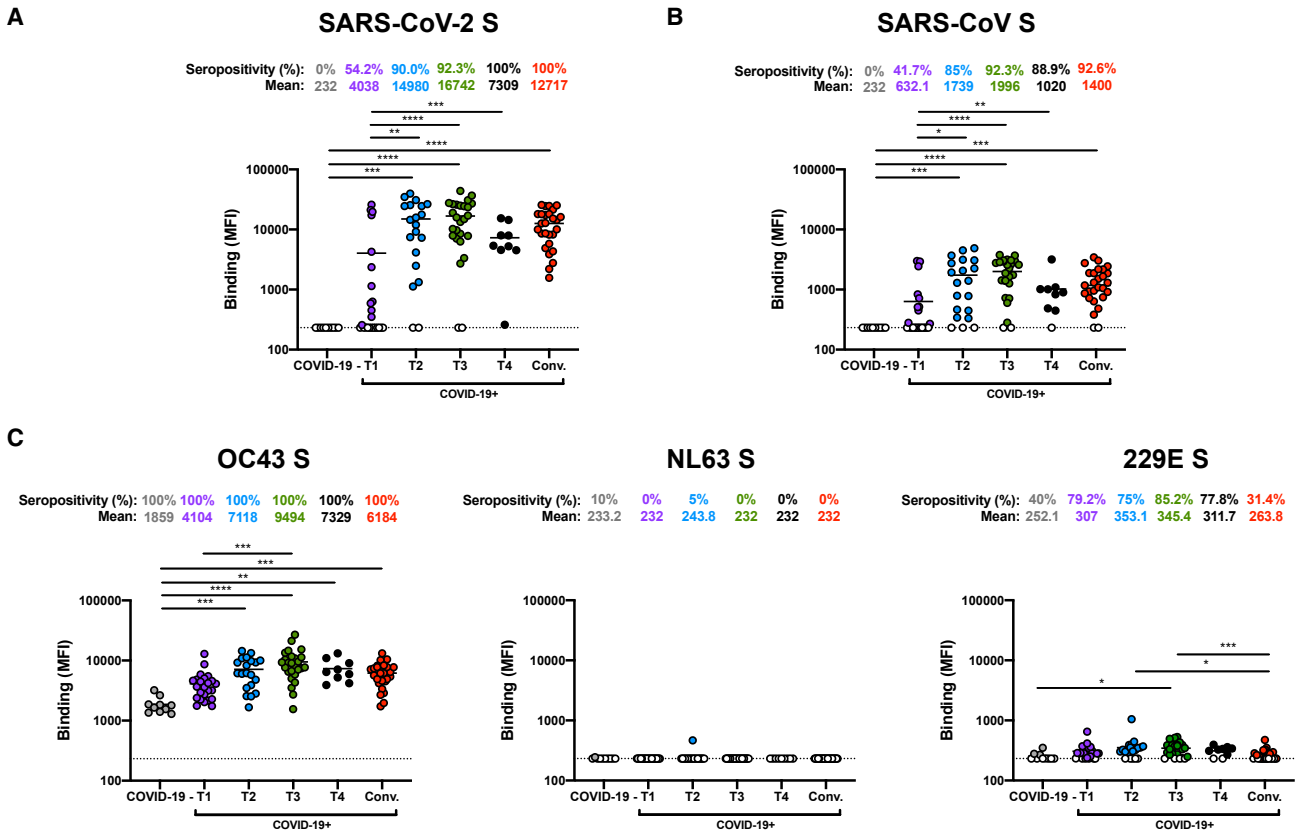

Figure 2. SARS-CoV-2 Infection Elicits Cross-Reactive Antibodies against Other Human *Betacoronavirus* Members

Cell-surface staining of 293T cells expressing full-length Spike (S) from different HCoVs: SARS-CoV-2 (A), SARS-CoV (B), OC43, NL63, and 229E (C) with samples from 10 COVID-19-negative or 106 COVID-19-positive patients at different stage of infection (T1, T2, T3, T4, and convalescent). The graphs shown represent the median fluorescence intensities (MFIs). Undetectable measures are represented as white symbols, and limits of detection are plotted. Error bars indicate means ± SEM. Statistical significance was tested using Kruskal-Wallis tests with a Dunn's post-test (*$p < 0.05$; **$p < 0.01$; ***$p < 0.001$; ****$p < 0.0001$).

between anti-S Abs and clinical parameters enhanced over time and was more prominent 3 weeks after the onset of the symptoms (T3 and T4). Admission to the ICU was significantly associated with levels of RBD-specific IgM and IgG and total SARS-CoV-2 S Abs (Figures 4A and S6A). The presence of respiratory symptoms was linked to higher levels of RBD-specific IgM and of neutralization activity against SARS-CoV-2 S (Figure 4A). Indeed, neutralizers (patients with detectable neutralization ID_{50} against SARS-CoV-2) were found to have stronger Ab responses and were more inclined to present respiratory symptoms (Figure S7).

DISCUSSION

This study helps us better understand the kinetics and persistence of humoral responses directed against SARS-CoV-2 (Figures 1, 2, and 3). Our results reveal that most infected individuals are able to elicit Abs directed against SARS-CoV-2 S within 2 weeks after symptom onset, and Abs persist after the resolution of the infection. Accordingly, all tested convalescent patients were found to be seropositive. As expected, RBD-specific IgM levels decreased during the study, whereas IgG remained relatively stable. Our results highlight how SARS-CoV-2 S, like other coronaviruses, appears to be relatively easily recognized by Abs present in sera from infected individuals. This was suggested to be linked to the higher processing of glycans than other type I fusion proteins, such as HIV-1 Env, influenza A hemagglutinin (HA), or filovirus glycoprotein (GP).[21,22] The ease of naturally elicited Abs to recognize the S might be associated with the low rate of somatic hypermutation observed in neutralizing Abs.[9] This low somatic hypermutation rate could in turn explain why most SARS-CoV-2-infected individuals are able to generate neutralizing Abs within only 2 weeks after infection (Figure 3). In contrast, the development of potent neutralizing Abs against HIV-1 Env usually requires 2–3 years of infection and requires a high degree of somatic hypermutation.[23] Nevertheless, in the case of SARS-CoV-2 infection, the neutralization capacity decreases significantly 6 weeks after the onset of symptoms, following a similar trend as anti-RBD IgM (Figures 1 and 3). Interestingly, anti-RBD IgM presented a stronger correlation with neutralization than IgG and IgA (Figures S4A and S4C), suggesting that at least part of the neutralizing activity is mediated by IgM. Our study is cross-sectional, but a series of longitudinal studies have also reported that neutralization activity against SARS-CoV-2 S wanes over time.[24–29] However, it remains unclear whether this reduced

CellPress
OPEN ACCESS

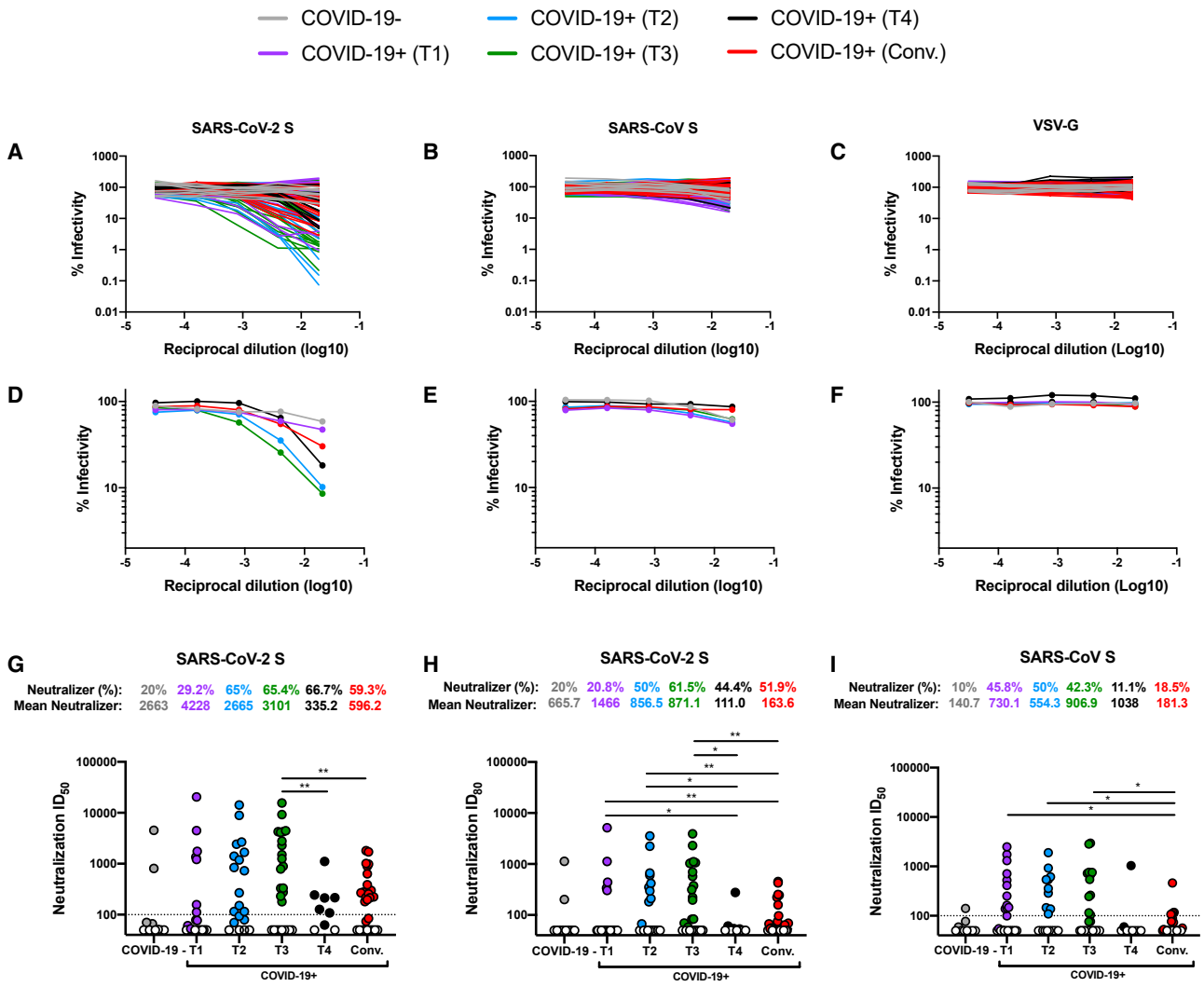

Figure 3. Anti-S Neutralizing Antibody Titers Decrease over Time

Pseudoviral particles coding for the luciferase reporter gene and bearing the glycoproteins SARS-CoV-2 S (A, D, G, and H), SARS-CoV S (B, E, and I), or VSV-G (C and F) were used to infect 293T-ACE2 cells. Pseudoviruses were incubated with serial dilutions of samples from 10 COVID-19-negative or 106 COVID-19-positive patients (T1, T2, T3, T4, and convalescent) at 37°C for 1 h prior to infection of 293T-ACE2 cells. Infectivity at each dilution was assessed in duplicate and is shown as the percentage of infection without sera for each glycoprotein. Neutralization half maximal inhibitory serum dilution (ID_{50}) (G and I) and ID_{80} (H) values were determined using a normalized non-linear regression using GraphPad Prism software. Undetectable measures are represented as white symbols. Neutralizer represent patients with an ID_{50} over 100 (G and I) or an ID_{80} (H). Statistical significance was tested using Mann-Whitney U tests (*$p < 0.05$; **$p < 0.01$).

level of neutralizing activity would remain sufficient to protect from re-infection.

Limitations of Study

A limitation of this study is its cross-sectional nature, which means that different patients were sampled for the different time point groups. However, we note that similar observations were obtained in longitudinal studies.[24–29] Moreover, the number of patients studied is relatively low, which can affect the power of the present study to determine the correlation between the levels of Ab response and clinical parameters. The potential links between serological and clinical parameters raised by our study will need to be further validated in clinical settings and in studies with a larger sample size.

STAR★METHODS

Detailed methods are provided in the online version of this paper and include the following:

- KEY RESOURCES TABLE
- RESOURCE AVAILABILITY
  - Lead Contact
  - Materials Availability
  - Data and Code Availability
- EXPERIMENTAL MODEL AND SUBJECT DETAILS
  - Ethics statement
  - Human subjects
  - Cell lines

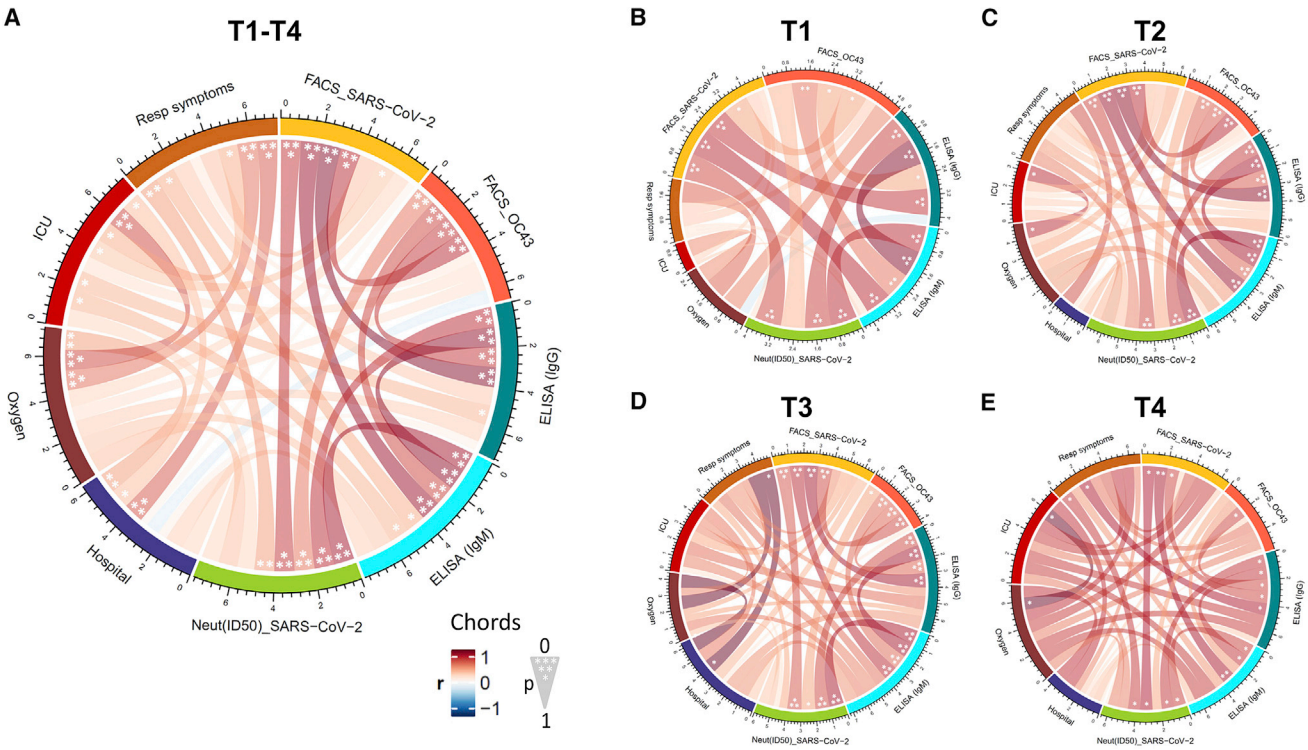

Figure 4. Association between Clinical and Serological Parameters in SARS-CoV-2-Infected Patients

Chord diagram illustrating the network of linear correlations among nine major serological and clinical factors for all acutely infected individuals (T1, T2, T3, and T4) (A) or at different time points (B–E). Chords are color-coded according to the magnitude of the correlation coefficient (r); chord width inversely corresponds to the p value. Asterisks indicate all statistically significant correlations within chords (*$p < 0.05$, **$p < 0.01$, ***$p < 0.005$). (A–E) Correlation analysis was done using nonparametric Spearman rank tests. The p values were adjusted for multiple comparisons using Holm-Sidak ($\alpha = 0.05$). Statistical comparisons of two parameters were done using Mann-Whitney U tests.

SUPPLEMENTAL INFORMATION

Supplemental Information can be found online at https://doi.org/10.1016/j.xcrm.2020.100126.

ACKNOWLEDGMENTS

The authors thank the CRCHUM BSL3 and Flow Cytometry Platforms for technical assistance. We thank Dr. Florian Krammer (Icahn School of Medicine at Mount Sinai, NY) for the plasmid expressing the SARS-CoV-2 RBD domain, Dr. Stefan Pöhlmann (Georg-August University, Germany) for the plasmids coding SARS-CoV S, SARS-CoV-2 S, and HCoV 229E and NL63 S glycoproteins, and Dr. M. Gordon Joyce (U.S. MHRP) for the monoclonal antibody CR3022. We also thank Danka K. Shank and Melina Bélanger Collard from the Laboratoire de Santé Publique du Québec for their help in preparing the specimens. The graphical abstract was prepared using images from BioRender.com. This work was supported by le Ministère de l'Économie et de l'Innovation du Québec, Programme de soutien aux organismes de recherche et d'innovation to A.F. and by the Fondation du CHUM. This work was also supported by Canada's COVID-19 Immunity Task Force (CITF), in collaboration with the Canadian Institutes of Health Research (CIHR) and a CIHR foundation grant #352417 to A.F. Development of SARS-CoV-2 reagents was partially supported by the NIAID Centers of Excellence for Influenza Research and Surveillance (CEIRS) contract HHSN272201400008C. A.F. is the recipient of Canada Research Chair on Retroviral Entry no. RCHS0235 950-232424. R.D. was supported by NIH grant R01 AI122953-05. M.C. is the recipient of a Tier II Canada Research Chair in Molecular Virology and Antiviral Therapeutics and an Ontario's Early Researcher Award. J. Prévost, G.B.-B., and S.P.A are supported by CIHR fellowships. R.G. is supported by a MITACS Accélération postdoctoral fellowship. M.S.M. was supported in part by a CIHR New Investigator Award, Ontario Early Researcher Award, CIHR COVID Rapid Response Funding, and the W. Garfield Weston Foundation Weston Family Microbiome Initiative. The funders had no role in study design, data collection and analysis, decision to publish, or preparation of the manuscript.

AUTHOR CONTRIBUTIONS

J. Prévost, J.R., B.S., R.B., M.R., and A.F. conceived the study. J. Prévost, J.R., and A.F. designed experimental approaches; J. Prévost, G.B.-B., R.G., A. Laumaea, J.R., S.P.A., G.G., M.B., S.D., T.T., J. Perreault, A. Lewin, R.D., R.B., M.R., and A.F. performed, analyzed, and interpreted the experiments; J. Prévost, G.B.-B., J.R., H.M., G.G.-L., H.D.S., M.S.M., M.D., P.J.T., G.T.G.M., M. Côté, and A.F. contributed novel reagents; N.G., M. Carrier, D.M., A.P., M.L., A.B., V.L., G.B., E.H., C.T., R.B., and M.R. collected clinical

samples; J. Prévost, J.R., and A.F. wrote the paper. Every author has read, edited, and approved the final manuscript.

DECLARATION OF INTERESTS

The authors declare no competing interests.

Received: June 12, 2020
Revised: August 20, 2020
Accepted: September 21, 2020
Published: September 30, 2020

REFERENCES

1. Hoffmann, M., Kleine-Weber, H., Schroeder, S., Kruger, N., Herrler, T., Erichsen, S., Schiergens, T.S., Herrler, G., Wu, N.H., Nitsche, A., et al. (2020). SARS-CoV-2 Cell Entry Depends on ACE2 and TMPRSS2 and Is Blocked by a Clinically Proven Protease Inhibitor. Cell *181*, 271–280.e278.
2. Walls, A.C., Xiong, X., Park, Y.J., Tortorici, M.A., Snijder, J., Quispe, J., Cameroni, E., Gopal, R., Dai, M., Lanzavecchia, A., et al. (2019). Unexpected Receptor Functional Mimicry Elucidates Activation of Coronavirus Fusion. Cell *176*, 1026–1039.e1015.
3. Shang, J., Ye, G., Shi, K., Wan, Y., Luo, C., Aihara, H., Geng, Q., Auerbach, A., and Li, F. (2020). Structural basis of receptor recognition by SARS-CoV-2. Nature *581*, 221–224.
4. Ou, X., Liu, Y., Lei, X., Li, P., Mi, D., Ren, L., Guo, L., Guo, R., Chen, T., Hu, J., et al. (2020). Characterization of spike glycoprotein of SARS-CoV-2 on virus entry and its immune cross-reactivity with SARS-CoV. Nat. Commun. *11*, 1620.
5. Zang, R., Gomez Castro, M.F., McCune, B.T., Zeng, Q., Rothlauf, P.W., Sonnek, N.M., Liu, Z., Brulois, K.F., Wang, X., Greenberg, H.B., et al. (2020). TMPRSS2 and TMPRSS4 promote SARS-CoV-2 infection of human small intestinal enterocytes. Sci. Immunol. *5*, eabc3582.
6. Wrapp, D., Wang, N., Corbett, K.S., Goldsmith, J.A., Hsieh, C.L., Abiona, O., Graham, B.S., and McLellan, J.S. (2020). Cryo-EM structure of the 2019-nCoV spike in the prefusion conformation. Science *367*, 1260–1263.
7. Walls, A.C., Park, Y.J., Tortorici, M.A., Wall, A., McGuire, A.T., and Veesler, D. (2020). Structure, Function, and Antigenicity of the SARS-CoV-2 Spike Glycoprotein. Cell *181*, 281–292.e286.
8. Yuan, M., Wu, N.C., Zhu, X., Lee, C.D., So, R.T.Y., Lv, H., Mok, C.K.P., and Wilson, I.A. (2020). A highly conserved cryptic epitope in the receptor binding domains of SARS-CoV-2 and SARS-CoV. Science *368*, 630–633.
9. Ju, B., Zhang, Q., Ge, J., Wang, R., Sun, J., Ge, X., Yu, J., Shan, S., Zhou, B., Song, S., et al. (2020). Human neutralizing antibodies elicited by SARS-CoV-2 infection. Nature *584*, 115–119.
10. Shi, R., Shan, C., Duan, X., Chen, Z., Liu, P., Song, J., Song, T., Bi, X., Han, C., Wu, L., et al. (2020). A human neutralizing antibody targets the receptor binding site of SARS-CoV-2. Nature *584*, 120–124.
11. Wu, Y., Wang, F., Shen, C., Peng, W., Li, D., Zhao, C., Li, Z., Li, S., Bi, Y., Yang, Y., et al. (2020). A noncompeting pair of human neutralizing antibodies block COVID-19 virus binding to its receptor ACE2. Science *368*, 1274–1278.
12. Murin, C.D., Wilson, I.A., and Ward, A.B. (2019). Antibody responses to viral infections: a structural perspective across three different enveloped viruses. Nat. Microbiol. *4*, 734–747.
13. Rouse, B.T., and Sehrawat, S. (2010). Immunity and immunopathology to viruses: what decides the outcome? Nat. Rev. Immunol. *10*, 514–526.
14. Stadlbauer, D., Amanat, F., Chromikova, V., Jiang, K., Strohmeier, S., Arunkumar, G.A., Tan, J., Bhavsar, D., Capuano, C., Kirkpatrick, E., et al. (2020). SARS-CoV-2 Seroconversion in Humans: A Detailed Protocol for a Serological Assay, Antigen Production, and Test Setup. Curr. Protoc. Microbiol. *57*, e100.
15. Amanat, F., Stadlbauer, D., Strohmeier, S., Nguyen, T.H.O., Chromikova, V., McMahon, M., Jiang, K., Arunkumar, G.A., Jurczyszak, D., Polanco, J., et al. (2020). A serological assay to detect SARS-CoV-2 seroconversion in humans. Nat. Med. *26*, 1033–1036.
16. Grzelak, L., Temmam, S., Planchais, C., Demeret, C., Huon, C., Guivel, F., Staropoli, I., Chazal, M., Dufloo, J., Planas, D., et al. (2020). SARS-CoV-2 serological analysis of COVID-19 hospitalized patients, pauci-symptomatic individuals and blood donors. medRxiv. https://doi.org/10.1101/2020.04.21.20068858.
17. Jaimes, J.A., André, N.M., Chappie, J.S., Millet, J.K., and Whittaker, G.R. (2020). Phylogenetic Analysis and Structural Modeling of SARS-CoV-2 Spike Protein Reveals an Evolutionary Distinct and Proteolytically Sensitive Activation Loop. J. Mol. Biol. *432*, 3309–3325.
18. Zhou, H., Chen, X., Hu, T., Li, J., Song, H., Liu, Y., Wang, P., Liu, D., Yang, J., Holmes, E.C., et al. (2020). A Novel Bat Coronavirus Closely Related to SARS-CoV-2 Contains Natural Insertions at the S1/S2 Cleavage Site of the Spike Protein. Curr. Biol. *30*, 2196–2203.e3.
19. Madu, I.G., Roth, S.L., Belouzard, S., and Whittaker, G.R. (2009). Characterization of a highly conserved domain within the severe acute respiratory syndrome coronavirus spike protein S2 domain with characteristics of a viral fusion peptide. J. Virol. *83*, 7411–7421.
20. Sterlin, D., Mathian, A., Miyara, M., Mohr, A., Anna, F., Claer, L., Quentric, P., Fadlallah, J., Ghillani, P., Gunn, C., et al. (2020). IgA dominates the early neutralizing antibody response to SARS-CoV-2. medRxiv. https://doi.org/10.1101/2020.06.10.20126532.
21. Watanabe, Y., Allen, J.D., Wrapp, D., McLellan, J.S., and Crispin, M. (2020). Site-specific glycan analysis of the SARS-CoV-2 spike. Science *369*, 330–333.
22. Watanabe, Y., Berndsen, Z.T., Raghwani, J., Seabright, G.E., Allen, J.D., Pybus, O.G., McLellan, J.S., Wilson, I.A., Bowden, T.A., Ward, A.B., and Crispin, M. (2020). Vulnerabilities in coronavirus glycan shields despite extensive glycosylation. Nat. Commun. *11*, 2688.
23. Sok, D., and Burton, D.R. (2018). Recent progress in broadly neutralizing antibodies to HIV. Nat. Immunol. *19*, 1179–1188.
24. Long, Q.X., Tang, X.J., Shi, Q.L., Li, Q., Deng, H.J., Yuan, J., Hu, J.L., Xu, W., Zhang, Y., Lv, F.J., et al. (2020). Clinical and immunological assessment of asymptomatic SARS-CoV-2 infections. Nat. Med. *26*, 1200–1204.
25. Yin, S., Tong, X., Huang, A., Shen, H., Li, Y., Liu, Y., Wu, C., Huang, R., and Chen, Y. (2020). Longitudinal anti-SARS-CoV-2 antibody profile and neutralization activity of a COVID-19 patient. J. Infect. *81*, e31–e32.
26. Zhang, G., Nie, S., Zhang, Z., and Zhang, Z. (2020). Longitudinal Change of Severe Acute Respiratory Syndrome Coronavirus 2 Antibodies in Patients with Coronavirus Disease 2019. J. Infect. Dis. *222*, 183–188.
27. Beaudoin-Bussières, G., Laumaea, A., Anand, S.P., Prévost, J., Gasser, R., Goyette, G., Medjahed, H., Perreault, J., Tremblay, T., Lewin, A., et al. (2020). Decline of humoral responses against SARS-CoV-2 Spike in convalescent individuals. bioRxiv. https://doi.org/10.1101/2020.07.09.194639.
28. Perreault, J., Tremblay, T., Fournier, M.-J., Drouin, M., Beaudoin-Bussières, G., Prévost, J., Lewin, A., Bégin, P., Finzi, A., and Bazin, R. (2020). Waning of SARS-CoV-2 RBD antibodies in longitudinal convalescent plasma samples within four months after symptom onset. Blood. https://doi.org/10.1182/blood.2020008367.
29. Ibarrondo, F.J., Fulcher, J.A., Goodman-Meza, D., Elliott, J., Hofmann, C., Hausner, M.A., Ferbas, K.G., Tobin, N.H., Aldrovandi, G.M., and Yang, O.O. (2020). Rapid Decay of Anti–SARS-CoV-2 Antibodies in Persons with Mild Covid-19. N. Engl. J. Med. *383*, e74.
30. Hofmann, H., Pyrc, K., van der Hoek, L., Geier, M., Berkhout, B., and Pöhlmann, S. (2005). Human coronavirus NL63 employs the severe acute respiratory syndrome coronavirus receptor for cellular entry. Proc. Natl. Acad. Sci. USA *102*, 7988–7993.
31. Hoffmann, M., Müller, M.A., Drexler, J.F., Glende, J., Erdt, M., Gützkow, T., Losemann, C., Binger, T., Deng, H., Schwegmann-Weßels, C., et al. (2013). Differential sensitivity of bat cells to infection by enveloped RNA

viruses: coronaviruses, paramyxoviruses, filoviruses, and influenza viruses. PLoS One *8*, e72942.

32. Lodge, R., Lalonde, J.P., Lemay, G., and Cohen, E.A. (1997). The membrane-proximal intracytoplasmic tyrosine residue of HIV-1 envelope glycoprotein is critical for basolateral targeting of viral budding in MDCK cells. EMBO J. *16*, 695–705.

33. Liu, Z., Pan, Q., Ding, S., Qian, J., Xu, F., Zhou, J., Cen, S., Guo, F., and Liang, C. (2013). The interferon-inducible MxB protein inhibits HIV-1 infection. Cell Host Microbe *14*, 398–410.

34. ter Meulen, J., van den Brink, E.N., Poon, L.L., Marissen, W.E., Leung, C.S., Cox, F., Cheung, C.Y., Bakker, A.Q., Bogaards, J.A., van Deventer, E., et al. (2006). Human monoclonal antibody combination against SARS coronavirus: synergy and coverage of escape mutants. PLoS Med. *3*, e237.

35. Tian, X., Li, C., Huang, A., Xia, S., Lu, S., Shi, Z., Lu, L., Jiang, S., Yang, Z., Wu, Y., and Ying, T. (2020). Potent binding of 2019 novel coronavirus spike protein by a SARS coronavirus-specific human monoclonal antibody. Emerg. Microbes Infect. *9*, 382–385.

36. Desforges, M., Desjardins, J., Zhang, C., and Talbot, P.J. (2013). The acetyl-esterase activity of the hemagglutinin-esterase protein of human coronavirus OC43 strongly enhances the production of infectious virus. J. Virol. *87*, 3097–3107.

37. R Core Team (2013). R: A language and environment for statistical computing (R Foundation for Statistical Computing).

38. R Studio Team (2015). RStudio: Integrated Development for R. (RStudio, Inc.). https://www.rstudio.com/.

39. Mauri, M., Elli, T., Caviglia, G., Uboldi, G., and Azzi, M. (2017). RAWGraphs: A Visualisation Platform to Create Open Outputs. In Proceedings of the 12th Biannual Conference on Italian SIGCHI Chapter (ACM), p. 5.

STAR★METHODS

KEY RESOURCES TABLE

REAGENT or RESOURCE	SOURCE	IDENTIFIER
Antibodies		
Mouse monoclonal anti-SARS-CoV-2 Spike (CR3022)	Dr M. Gordon Joyce	RRID:AB_2848080
Mouse monoclonal anti-OC43 Spike (4.3E4)	Desforges et al.[36]	RRID:AB_2847964
Goat polyclonal anti-human ACE2	R&D systems	Cat# AF933
Goat anti-Human IgG (H+L) Cross-Adsorbed Secondary Antibody, Alexa Fluor 647	Invitrogen	Cat# A21445; RRID:AB_2535862
Donkey anti-Goat IgG (H+L) Cross-Adsorbed Secondary Antibody, Alexa Fluor 647	Invitrogen	Cat# A21447; RRID:AB_2535864
Goat anti-Human IgG Fc Cross-Adsorbed Secondary Antibody, HRP	Invitrogen	Cat# A18823; RRID:AB_2535600
Peroxidase AffiniPure Goat Anti-Human IgM, Fc5μ fragment specific	Jackson ImmunoResearch	Cat# 109-035-129; RRID:AB_2337588
Peroxidase AffiniPure Goat Anti-Human Serum IgA, α chain specific	Jackson ImmunoResearch	Cat# 109-035-011; RRID:AB_2337580
Biological Samples		
Human Sera/Plasma from SARS-CoV-2-infected or uninfected donors	This paper	N/A
Chemicals, Peptides, and Recombinant Proteins		
Dulbecco's modified Eagle's medium (DMEM)	Wisent	Cat# 319-005-CL
Penicillin/streptomycin	Wisent	Cat# 450-201-EL
Fetal bovine serum (FBS)	VWR	Cat# 97068-085
Tris-buffered saline (TBS)	Thermo Fisher Scientific	Cat# BP24711
Bovine Serum Albumin (BSA)	BioShop	Cat# ALB001.100
Phosphate buffered saline (PBS)	Wisent	Cat# 311-010-CL
Western Lightning Plus-ECL, Enhanced Chemiluminescence Substrate	Perkin Elmer Life Sciences	Cat# NEL105001EA
Tween20	Thermo Fisher Scientific	Cat# BP337-500
Puromycin dihydrochloride	Millipore Sigma	Cat# P8833
Passive lysis buffer	Promega	Cat# E1941
FreeStyle 293F expression medium	ThermoFisher Scientific	Cat# 12338002
ExpiFectamine 293 transfection reagent	ThermoFisher Scientific	Cat# A14525
Ni-NTA agarose	Invitrogen	Cat# R90110
D-Luciferin potassium salt	Thermo Fisher Scientific	Cat# L2916
LIVE/DEAD Fixable AquaVivid Cell Stain	Thermo Fisher Scientific	Cat# L34957
Formaldehyde 37%	Thermo Fisher Scientific	Cat# F79-500
Critical Commercial Assays		
Alexa Fluor 594 Protein Labeling Kit	Invitrogen	Cat# A10239
Experimental Models: Cell Lines		
HEK293T human embryonic kidney cells	ATCC	Cat# CRL-3216; "RRID:CVCL_0063
FreeStyle 293F Cells	ThermoFisher Scientific	Cat# R79007; RRID:CVCL_D603
293T-ACE2	This paper	N/A
Recombinant DNA		
pCG1-SARS-CoV-2 Spike	Hoffmann et al.[1]	N/A
pCG1-SARS-CoV Spike	Hoffmann et al.[31]	N/A
pCAGGS-229E Spike	Hofmann et al.[31]	N/A

(*Continued on next page*)

Continued

REAGENT or RESOURCE	SOURCE	IDENTIFIER
pCAGGS-NL63 Spike	Hofmann et al.[31]	N/A
pCAGGS-OC43 Spike	This paper	N/A
pCAGGS-SARS-CoV-2 RBD	Amanat et al.[15]	N/A
pcDNA3.1-OC43 RBD	This paper	N/A
pNL4.3 R-E- Luc	NIH AIDS Reagent Program	Cat# 3418
pSVCMV-IN-VSV-G	Lodge et al.[32]	N/A
pLenti-C-mGFP-P2A-Puro-ACE2	OriGene	Cat# RC208442L4
Lentiviral packaging plasmids (pLP1, pLP2)	Liu et al.[33]	N/A
pIRES-GFP vector	Dr. Mark Brockman	N/A
Software and Algorithms		
FlowJo v10	Tree Star	https://www.flowjo.com/
GraphPad Prism v8	GraphPad	https://www.graphpad.com/
R v3	R	https://www.r-project.org/
RStudio v1	RStudio	https://www.rstudio.com/
Microsoft Excel v16	Microsoft Office	https://www.microsoft.com/en-ca/microsoft-365/excel
Other		
BD LSR II Flow Cytometer	BD Biosciences	N/A
TriStar LB 942 Microplate Reader	Berthold Technologies	N/A

RESOURCE AVAILABILITY

Lead Contact

Further information and requests for resources and reagents should be directed to and will be fulfilled by the Lead Contact, Andrés Finzi (andres.finzi@umontreal.ca).

Materials Availability

All unique reagents generated in this study are available from the Lead Contact with a completed Materials Transfer Agreement.

Data and Code Availability

Further information and requests for resources and reagents should be directed to and will be fulfilled by the Lead Contact Author (andres.finzi@umontreal.ca).

EXPERIMENTAL MODEL AND SUBJECT DETAILS

Ethics statement

All work was conducted in accordance with the Declaration of Helsinki in terms of informed consent and approval by an appropriate institutional board. In addition, this study was conducted in accordance with the rules and regulations concerning ethical reviews in Quebec, particularly those specified in the Civil Code (http://legisquebec.gouv.qc.ca/fr/ShowDoc/cs/CCQ-1991) and in subsequent IRB practice. Informed Consent was obtained for all participating subjects and the study was approved by Quebec Public health authorities. Convalescent plasmas were obtained from donors who consented to participate in this research project (REB # 2020-004). The donors were recruited by Héma-Québec and met all donor eligibility criteria for routine apheresis plasma donation, plus two additional criteria: previous confirmed COVID-19 infection and complete resolution of symptoms for at least 14 days. Plasma samples from COVID- children were obtained from donors enrolled in a research protocol from CHU Ste-Justine (REB #3195).

Human subjects

The present study aims to determine the kinetics of the humoral response following SARS-CoV-2 infection. All available samples from adults diagnosed with acute SARS-CoV-2 infection by PCR collected at the time of the study were analyzed. No specific criteria such as number of patients (sample size), clinical or demographic were used for inclusion, beyond PCR confirmed SARS-CoV-2 infection in adults. Subjects were allocated to the different groups (T1-T4) based on the number of days post-symptoms onset the sample was collected. A summary of demographic parameters for all COVID+ subjects is included in Table S1. The overall findings of this study were found to be independent of the age and sex of the subjects (see Figure S5).

Cell lines

293T human embryonic kidney cells (obtained from ATCC) were maintained at 37°C under 5% CO_2 in Dulbecco's modified Eagle's medium (DMEM) (Wisent) containing 5% fetal bovine serum (VWR) and 100 μg/ml of penicillin-streptomycin (Wisent). For the generation of 293T cells stably expressing human ACE2, transgenic lentiviruses were produced in 293T using a third-generation lentiviral vector system. Briefly, 293T cells were co-transfected with two packaging plasmids (pLP1 and pLP2), an envelope plasmid (pSVCMV-IN-VSV-G) and a lentiviral transfer plasmid coding for human ACE2 (pLenti-C-mGFP-P2A-Puro-ACE2) (OriGene). Forty-eight hours post-transfection, supernatant containing lentiviral particles was used to infect more 293T cells in presence of 5μg/mL polybrene. Stably transduced cells were enriched upon puromycin selection. 293T-ACE2 cells were then cultured in a medium supplemented with 2 μg/ml of puromycin (Millipore Sigma).

METHOD DETAILS

Plasmids

The plasmids expressing the human coronavirus Spikes of SARS-CoV-2, SARS-CoV, NL63 and 229E were previously reported.[1,30,31] The OC43 Spike with an N-terminal 3xFlag tag and C-terminal 17 residue deletion was cloned into pCAGGS following amplification of the spike gene from pB-Cyst-3FlagOC43SC17 (kind gift of James M. Rini, University of Toronto, ON, Canada). The plasmid encoding for SARS-CoV-2 S RBD (residues 319-541) fused with a hexahistidine tag was reported elsewhere.[15] The sequence for the HCoV OC43 RBD was obtained from the UniProt Protein Database (P36334 SPIKE_CVHOC). An N-terminal 13aa signal sequence and a C-terminal His-tag were added for downstream protein purification. Mammalian cell codon optimization was performed using the GenScript GenSmart Codon Optimization Tool. The RBD gene was synthesized by GenScript and cloned into the pcDNA3.1 plasmid between EcoRI and XhoI sites. The vesicular stomatitis virus G (VSV-G)-encoding plasmid (pSVCMV-IN-VSV-G) was previously described.[32] The lentiviral packaging plasmids pLP1 and pLP2, coding for HIV-1 gag/pol and rev respectively, were reported elsewhere.[33] The transfer plasmid (pLenti-C-mGFP-P2A-Puro-ACE2) encoding for human angiotensin converting enzyme 2 (ACE2) fused with a mGFP C-terminal tag and a puromycin selection marker was purchased from OriGene.

Protein expression and purification

FreeStyle 293F cells (Thermo Fisher Scientific) were grown in FreeStyle 293F medium (Thermo Fisher Scientific) to a density of 1 × 10^6 cells/mL at 37°C with 8% CO_2 with regular agitation (150 rpm). Cells were transfected with a plasmid coding for SARS-CoV-2 S RBD or OC43 S RBD using ExpiFectamine 293 transfection reagent, as directed by the manufacturer (Thermo Fisher Scientific). One week later, cells were pelleted and discarded. Supernatants were filtered using a 0.22 μm filter (Thermo Fisher Scientific). The recombinant RBD proteins were purified by nickel affinity columns, as directed by the manufacturer (Invitrogen). The RBD preparations were dialyzed against phosphate-buffered saline (PBS) and stored in aliquots at −80°C until further use. To assess purity, recombinant proteins were loaded on SDS-PAGE gels and stained with Coomassie Blue. For cell-surface staining, RBD proteins were fluorescently labeled with Alexa Fluor 594 (Invitrogen) according to the manufacturer's protocol.

Sera and antibodies

Sera from SARS-CoV-2-infected and uninfected donors were collected, heat-inactivated for 1 hour at 56°C and stored at −80°C until ready to use in subsequent experiments. The monoclonal antibodies CR3022 and 4.3E4 were used as positive controls in ELISA assays and were previously described.[8,34–36] Horseradish peroxidase (HRP)-conjugated antibody specific for the Fc region of human IgG (Invitrogen), for the Fc region of human IgM (Jackson ImmunoReasearch) or for the Fc region of human IgA (Jackson ImmunoResearch) were used as secondary antibodies to detect sera binding in ELISA experiments. Alexa Fluor-647-conjugated goat anti-human IgG (H+L) Abs (Invitrogen) were used as secondary antibodies to detect sera binding in flow cytometry experiment. Polyclonal goat anti-ACE2 (R&D systems) and Alexa Fluor-conjugated donkey anti-goat IgG Abs (Invitrogen) were used to detect cell-surface expression of human ACE2.

ELISA assay

Recombinant SARS-CoV-2 S RBD proteins (or OC43 S RBD proteins) (2.5 μg/ml), or bovine serum albumin (BSA) (2.5 μg/ml) as a negative control, were prepared in PBS and were adsorbed to plates (MaxiSorp; Nunc) overnight at 4°C. Coated wells were subsequently blocked with blocking buffer (Tris-buffered saline [TBS] containing 0.1% Tween20 and 2% BSA) for 1h at room temperature. Wells were then washed four times with washing buffer (Tris-buffered saline [TBS] containing 0.1% Tween20). CR3022 mAb (50ng/ml) or sera from SARS-CoV-2-infected or uninfected donors (1/100; 1/250; 1/500; 1/1000; 1/2000; 1/4000) were diluted in blocking buffer and incubated with the RBD-coated wells for 1h at room temperature. Plates were washed four times with washing buffer followed by incubation with secondary Abs (diluted in blocking buffer) for 1h at room temperature, followed by four washes. HRP enzyme activity was determined after the addition of a 1:1 mix of Western Lightning oxidizing and luminol reagents (Perkin Elmer Life Sciences). Light emission was measured with a LB942 TriStar luminometer (Berthold Technologies). Signal obtained with BSA was subtracted for each serum and were then normalized to the signal obtained with CR3022 mAb present in each plate. Alternatively, the signal obtained with each serum on OC43 RBD was normalized with the signal obtained with 4.3E4 mAb present in each

plate. The seropositivity threshold was established using the following formula: mean RLU of all COVID-19 negative sera normalized to CR3022 (or 4.3E4) + (3 standard deviations of the mean of all COVID-19 negative sera).

Flow cytometry analysis of cell-surface staining

Using the standard calcium phosphate method, 10 μg of Spike expressor and 2 μg of a green fluorescent protein (GFP) expressor (pIRES-GFP; kindly provided by Dr Mark Brockman, Simon Fraser University) was transfected into 2×10^6 293T cells. At 48h post transfection, 293T cells were stained with sera from SARS-CoV-2-infected or uninfected individuals (1:250 dilution). The percentage of transfected cells (GFP+ cells) was determined by gating the living cell population based on the basis of viability dye staining (Aqua Vivid, Invitrogen). Samples were acquired on a LSRII cytometer (BD Biosciences, Mississauga, ON, Canada) and data analysis was performed using FlowJo v10.5.3 (Tree Star, Ashland, OR, USA). The seropositivity threshold was established using the following formula: (mean of all COVID-19 negative sera + (3 standard deviation of the mean of all COVID-19 negative sera) + inter-assay coefficient of variability).

Virus neutralization assay

Target cells were infected with single-round luciferase-expressing lentiviral particles. Briefly, 293T cells were transfected by the calcium phosphate method with the lentiviral vector pNL4.3 R-E- Luc (NIH AIDS Reagent Program) and a plasmid encoding for SARS-CoV-2 Spike, SARS-CoV Spike or VSV-G at a ratio of 5:4. Two days post-transfection, cell supernatants were harvested and stored at –80°C until use. 293T-ACE2 target cells were seeded at a density of 1×10^4 cells/well in 96-well luminometer-compatible tissue culture plates (Perkin Elmer) 24h before infection. Recombinant viruses in a final volume of 100 μL were incubated with the indicated sera dilutions (1/50; 1/250; 1/1250; 1/6250; 1/31250) for 1h at 37°C and were then added to the target cells followed by incubation for 48h at 37°C; cells were lysed by the addition of 30 μL of passive lysis buffer (Promega) followed by one freeze-thaw cycle. An LB942 TriStar luminometer (Berthold Technologies) was used to measure the luciferase activity of each well after the addition of 100 μL of luciferin buffer (15mM $MgSO_4$, 15mM KPO_4 [pH 7.8], 1mM ATP, and 1mM dithiothreitol) and 50 μL of 1mM d-luciferin potassium salt (ThermoFisher Scientific). The neutralization half-maximal inhibitory dilution (ID_{50}) or the neutralization 80% inhibitory dilution (ID_{80}) represents the sera dilution to inhibit 50% or 80% of the infection of 293T-ACE2 cells by recombinant viruses bearing the indicated surface glycoproteins.

QUANTIFICATION AND STATISTICAL ANALYSIS

Software Scripts and Visualization

Correlograms were generated using the corrplot package in program R and R Studio.[37,38] Dendrograms were calculated using the dendPlot function and hclust method, or as implemented in the heatmap package in R. Chord diagrams were generated in R and R Studio based on the circlize and ComplexHeatmap package, as recently described. For time series, area graphs were generated using RawGraphs with DensityDesign interpolation and the implemented normalization using vertically un-centered values.[39] Forrest plots and calculations of fold change, significance (Mann-Whitney) and adjusted P values (Holm-Sidak) were done using Excel and Prism v8.2.0. The confidence interval of a quotient of two means was calculated based on the Fieller method using GraphPad QuickCalcs.

Statistical analyses

Statistics were analyzed using GraphPad Prism version 8.0.2 (GraphPad, San Diego, CA, (USA). Every dataset was tested for statistical normality and this information was used to apply the appropriate (parametric or nonparametric) statistical test. P values < 0.05 were considered significant; significance values are indicated as * $p < 0.05$, ** $p < 0.01$, *** $p < 0.001$, **** $p < 0.0001$. Corrections for multiple comparisons were performed with the Holm-Sidak method.